JCTC Journal of Chemical Theory and Computation

Polarizable Molecular Dynamics Simulation of Zn(II) in Water Using the AMOEBA Force Field

Johnny C. Wu,[†] Jean-Philip Piquemal,*[,‡,§] Robin Chaudret,[‡,§] Peter Reinhardt,[‡,§] and Pengyu Ren*[,†]

Department of Biomedical Engineering, University of Texas at Austin, Austin, Texas 78712-1062, UPMC Univ. Paris 06, UMR 7616, Laboratoire de Chimie Théorique, case courrier 137, 4 place Jussieu, F-75005, Paris, France, and CNRS, UMR 7616, Laboratoire de Chimie Théorique, case courrier 137, 4 place Jussieu, F-75005, Paris, France

Received February 15, 2010

Abstract: The hydration free energy, structure, and dynamics of the zinc divalent cation are studied using a polarizable force field in molecular dynamics simulations. Parameters for the Zn^{2+} are derived from gas-phase *ab initio* calculation of the Zn^{2+}−water dimer. The Thole-based dipole polarization is adjusted on the basis of the constrained space orbital variations (CSOV) calculation, while the symmetry adapted perturbation theory (SAPT) approach is also discussed. The vdW parameters of Zn^{2+} have been obtained by comparing the AMOEBA Zn^{2+}−water dimerization energy with results from several theory levels and basis sets over a range of distances. Molecular dynamics simulations of Zn^{2+} solvation in bulk water are subsequently performed with the polarizable force field. The calculated first-shell water coordination number, water residence time, and free energy of hydration are consistent with experimental and previous theoretical values. The study is supplemented with extensive reduced variational space (RVS) and electron localization function (ELF) computations in order to unravel the nature of the bonding in $Zn^{2+}(H_2O)_n$ ($n = 1, 6$) complexes and to analyze the charge transfer contribution to the complexes. Results show that the importance of charge transfer decreases as the size of the Zn−water cluster grows due to anticooperativity and to changes in the nature of the metal−ligand bonds. Induction could be dominated by polarization when the system approaches the condensed phase and the covalent effects are eliminated from the Zn(II)−water interaction. To construct an "effective" classical polarizable potential for Zn^{2+} in bulk water, one should therefore avoid overfitting to the *ab initio* charge transfer energy of the Zn^{2+}−water dimer. Indeed, in order to avoid overestimation of the condensed-phase many-body effects, which is crucial to the transferability of polarizable molecular dynamics, charge transfer should not be included within the classical polarization contribution and should preferably be either incorporated into the pairwise van der Waals contribution or treated explicitly.

I. Introduction

Since the 1940s, we have begun to appreciate that specific biological functions critically depend on the presence of zinc.[1] Moreover, its divalent cation, Zn^{2+}, plays an important role in many metalloenzymes by acting directly as a structural element in proteins such as Zn-fingers[2] or by serving as a cofactor.[3] Due to zinc's soft character and the subtle nature of its interactions with the biological environment,[4] quantum mechanics (QM) is usually the primary methodology for the study of Zn^{2+}−metalloproteins.[5−7] Of course, such an approach is limited to "static" structures of relatively small biomimetic models due to the high computational demands

* Corresponding authors. E-mail: jpp@lct.jussieu.fr (J.-P.P.), pren@mail.utexas.edu (P.R.).
[†] University of Texas at Austin.
[‡] UPMC Univ. Paris.
[§] CNRS.

10.1021/ct100091j
Published on Web 06/11/2010

by state of the art QM approaches. Hybrid methods that combine QM and molecular mechanics (QM/MM)[8−11] offer the possibility to treat the whole protein on longer time scales. Nevertheless, if one is interested in the dynamical behavior of Zn^{2+} complexes, available methods remain sparse. Traditional fixed charge force fields are unable to capture the interactions between Zn^{2+} and its ligands, or even to keep the Zn^{2+} "in place", unless using artificial bonds[12] or extra charge sites.[13] Recent studies based on quasi-chemical theory have shown the importance of polarization in ion hydration.[14,15]

As an alternative to QM, anisotropic polarizable molecular mechanics (APMM) methods, such as SIBFA (sum of interactions between fragments *ab initio* computed)[16,17] and AMOEBA,[18] have been developed in recent years. Such techniques are computationally more efficient and provide potential energy surfaces in close agreement with QM. For the specific case of Zn^{2+}, SIBFA, which treats both polarization and charge transfer contributions, has been shown to be particularly accurate and has enabled the study of large biological systems.[16,19−23] As SIBFA's extension to MD is under development, AMOEBA has already been extensively tested in simulations of various systems including proteins[24−26] and has been shown to be particularly suited for the computation of dynamical properties of metal cations of biological interest.[19−22,27−29]

In this contribution, as a first step toward modeling Zn^{2+} metalloenzymes, we will show that AMOEBA is able to accurately capture Zn^{2+} solvation properties. In the first part of this work, we will detail the parametrization process which is grounded on gas phase *ab initio* calculations following a "bottom-up" approach.[16] The application of energy decomposition analyses (EDA) techniques[17] such as the constrained space orbital variations (CSOV),[30] reduced variational space (RVS),[31] and symmetry adapted perturbation theory (SAPT)[32] to AMOEBA's parametrization will be discussed. Moreover, such approaches are used to evaluate the importance of the charge transfer contribution. The nature of the interaction of Zn^{2+} with water will be investigated using the electron localization function (ELF)[33] topological analysis.[34] In the second part, we will perform extensive condensed-phase simulations using AMOEBA to compute Zn^{2+} solvation properties such as the ion−water radial distribution function (RDF), water residence times, and the coordination number, as well as the solvation free energy. Comparison is made to experimental results as well as other divalent cations that have previously been studied using AMOEBA.

II. Computational Details

Gas Phase *ab Initio* Calculations. The intermolecular interaction energies of $Zn^{2+}-H_2O$ at various separations were calculated using Gaussian 03[35] at the MP2(full) level. Basis set superposition error (BSSE) correction was included in the binding energy. The geometry of the previously derived AMOEBA water model was applied.[36,37] The aug-cc-pVTZ basis set[38] was employed for water and the 6-31G(2d,2p) basis set for the Zn^{2+} cation. Post-Hartree−Fock symmetry adapted perturbation theory (SAPT) calculations were performed with the same basis sets at the MP2 and CCSD levels using the *Dalton* package[38] and SAPT 96.[39] CSOV polarization energy calculations were performed using a modified version[40] of HONDO95.3[40] with the B3LYP methods[41,42] using the above basis sets. The Zn^{2+} atomic polarizability was computed using Gaussian 03 at the MP2(full)/6-31G** level.

Additional energy decomposition analysis was performed on the zinc hydrated cluster with the reduced variational space (RVS) scheme as implemented in the GAMESS[43] software. The RVS energy decomposition computations were performed at the Hartree−Fock (HF) level using the CEP 4−31G(2d) basis set[44] augmented with two diffuse 3d polarization functions on heavy atoms (double-ζ-quality pseudopotential) and at the aug-cc-pVTZ basis set level (6-31G** for Zn(II)).

Electron Localization Function Analysis (ELF). In the framework of the ELF[33,45] topological analysis,[34] the molecular space is divided into a set of molecular volumes or regions (the so-called "basins") localized around maxima (attractors) of the vector field of the scalar ELF function. The ELF function can be interpreted as a signature of the electronic-pair distribution, and ELF is defined to have values restricted between 0 and 1 to facilitate its computation on a 3D grid and its interpretation. The core regions can be determined (if $Z > 2$) for any atom A. Regions associated to lone pairs are referred to as V(A), and bonding regions denoting chemical bonds are denoted V(A,B). The approach offers an evaluation of the basin electronic population as well as an evaluation of local electrostatic moments. It is also important to point out that metal cations exhibit a specific topological signature in the electron localization of their density interacting with ligands according to their "soft" or "hard" character. Indeed, a metal cation can split its outer-shell density (the so-called subvalent domains or basins) according to its capability to form a partly covalent bond involving charge transfer.[46] More details about the ELF function and its application to biology can be found in a recent review.[47] All computations have been performed using a modified version[48] of the Top-Mod package.[49]

III. Parameterization and Free Energy Simulations

Use of CSOV and SAPT Energy Decompositions Schemes. Following a procedure that has already shown success with Ca(II) and Mg(II),[29] the Zn^{2+} cation is parametrized by first matching the distance dependence of AMOEBA polarization energies of the ion−water dimer in the gas phase with reference *ab initio* CSOV polarization energy results. In order to supplement the CSOV decomposition, we have also performed SAPT computations (available in the Supporting Information). It is important to note that, despite the fact that SAPT could be expected to be the reference analysis offering up to CCSD correlation corrections to compute the contributions, a close examination of the results clearly shows that SAPT has problems with converging to the supermolecular interaction energy. A similar trend has recently been observed by Rayon et al.[6] It appears that difficulty with convergence is mainly due to the second order induction term, which consists of both

polarization and charge transfer energies.[17] Such a problem is not new, as Claverie[50] and then Kutzelnigg[51] showed 30 years ago that the convergence of the SAPT expansion was not guaranteed. As in recent studies on water,[52] the discrepancy of total SAPT energies compared to supermolecular interaction energy results can be traced back to the importance of the third order induction correction. Their inclusion clearly enhances the binding energy and could therefore improve SAPT results. We reported here extensive SAPT results in a detailed Supporting Information section dealing with the Zn^{2+}−water complex. As one can see from the Supporting Information, at the Hartree−Fock level, the SAPT approximation tends not to converge at short-range, the total SAPT energy being far from the supermolecular HF value. Around the equilibrium (Zn^{2+}−O = 2.0 Å), and beyond, this discrepancy tends to diminish, becoming negligible at long range. However, since the AMOEBA force field is based on the reproduction of supermolecular interaction energies, we need short-range induction data in order to refine the parameters. Moreover, as SAPT induction embodies both charge transfer and polarization, we cannot fit directly the sole "polarization only" Thole model to these values. Consequently, for the present purpose of AMOEBA's fitting, we have limited our use of the SAPT results to a comparison of the accuracy of AMOEBA's Halgren 14−7 van der Waals function[53] at long-range directly to the sum of the SAPT exchange-repulsion, dispersion, and exchange-dispersion. Such a fit is reflected in the good agreement between the AMOEBA and ab initio total interaction energy at long range (see Figure 5).

In summary, we fit AMOEBA's polarization contribution (the damping factor "a" in the next section) to the CSOV results. The remaining induction contribution (charge transfer) will be included in the van der Waals term as a result of matching the total binding energy of AMOEBA to that of QM. In the absence of an explicit charge transfer term, such a strategy is justified, as the charge transfer contribution is notably smaller in magnitude compared to polarization[4,16,22,23] and a good percentage of it (namely the two-body part) could be accurately included within AMOEBA's van der Waals term assuming that many-body charge transfer is not the driving force of Zn(II) solvation dynamics. The validity of such an assumption and the applicability of the present parametrization scheme to Zn^{2+} will be discussed in the first section of the discussion.

AMOEBA Calculation Details. The AMOEBA polarizable force field[28,36,37] is used to study the solvation dynamics of Zn(II). Hence, the electrostatic term of the model accounts for polarizability via atomic dipole induction:

$$\mu_{i,\alpha}^{\mathrm{ind}} = \alpha_i\left(\sum_{\{j\}} T_{\alpha}^{ij} M_j + \sum_{\{j'\}} T_{\alpha\beta}^{ij'} \mu_{j',\beta}^{\mathrm{ind}}\right) \text{ for } \alpha,\beta = 1,2,3$$

where $M_j = [q_j,\mu_{j,1},\mu_{j,2},\mu_{j,3},...]^T$ are the permanent charge, dipole, and quadrupole moments and $T_{\alpha}^{ij} = [T_{\alpha},T_{\alpha 1},T_{\alpha 2},T_{\alpha 3},...]$ is the interaction matrix between atoms i and j. The Einstein convention is used to sum over indices α and β. The atomic polarizability, α_i, is parametrized for the zinc cation in this work. Note that the first term within the parentheses corresponds to the polarization field due to permanent multipoles, while the second term corresponds to the polarization field due to induced dipoles produced at the other atoms.

The dipole polarization is damped via smeared charge distributions as proposed by Thole:[54]

$$\rho = \frac{3a}{4\pi}\exp(-au^3)$$

where $u = R_{ij}/(\alpha_i\alpha_j)^{1/6}$ is the effective distance between atoms i and j. The scalar a, a dimensionless parameter corresponding to the width of the smeared charge distribution, is parametrized to be 0.39 for water[36] and monovalent ions.[55] A previous study suggested that, for monovalent ions, AMOEBA is able to reproduce *ab initio* MP2 correlated results and hydration enthalpies without modifying the damping factor. However, since divalent ions, such as Ca^{2+} and Mg^{2+},[28,29] require a wider charge distribution in order to agree with QM ion−water dimer energy, smaller values of a were assigned. The value for Zn^{2+} is also adjusted from 0.39 and is compared with those of Ca^{2+} and Mg^{2+} below.

The repulsion−dispersion (van der Waals) interaction is represented by a buffered 14−7 function:[53]

$$U_{ij}^{\mathrm{buff}} = \varepsilon_{ij}\left(\frac{1+\delta}{\rho_{ij}+\delta}\right)^{n-m}\left(\frac{1+\gamma}{\rho_{ij}^{m}+\gamma} - 2\right)$$

where ε_{ij} is the potential well depth. In addition, ρ_{ij} is R_{ij}/R_{ij}^0, where R_{ij} is the separation distance between atoms i and j, and R_{ij}^0 is the minimum energy distance. Following Halgren, we used fixed values of $n = 14$, $m = 7$, $\delta = 0.07$, and $\gamma = 0.12$. The values for R_{ij}^0 and ε_{ij} are parametrized. The polarizable water model as developed by Ren and Ponder[36] is employed in this study.

With water geometry fixed, the Zn^{2+}−O distances were varied between 1.5 and 5 Å. The damping factor "a" was adjusted so that the AMOEBA polarization energy matched the CSOV values as much as possible. Next, parameters for the van der Waals interaction, R^0 (radius) and ε (well-depth), were derived by comparing the total ion−water binding energy computed by AMOEBA to the *ab initio* values at various distances. For interactions between different types of atoms, these parameters undergo combination rules as described by Ponder et al.[26] The binding energies were computed as the total energy less the isolated water and ion energies at an infinite separation distance.

Molecular dynamics simulations were performed via the TINKER 5 package[56] to compute the solvation free energy of Zn^{2+}. Fourteen independent simulations were first performed to "grow" the Zn vdW particle by gradually varying $R(\lambda) = \lambda(R_{\mathrm{final}})$ and $\varepsilon(\lambda) = \lambda(\varepsilon_{\mathrm{final}})$, where λ = (0.0, 0.0001, 0.001, 0.1, 0.2, 0.3, 0.4, 0.5, 0.6, 0.7, 0.8, 0.9, 1.0). Subsequently, 30 simulations were performed to "grow" the (+2) charge of Zn^{2+} along with its polarizability such that $q(\lambda') = \lambda'(q_{\mathrm{final}})$ and $\alpha(\lambda') = \lambda'(\alpha_{\mathrm{final}})$, where λ' = (0.0, 0.1, 0.2, 0.3, 0.325, 0.350, 0.375, 0.400, 0.425, 0.450, 0.475, 0.500, ..., 1.0). The long-range electrostatics are modeled with particle-mesh Ewald summation for atomic multipoles with a cutoff of 7 Å in real space and 0.5 Å spacing and a fifth-order spline in reciprocal space.[57] The convergence

Table 1. Polarization Energy and Charge Transfer Energy from Restricted Variational Space (RVS) Energy Decomposition of Zn^{2+} in the Presence of Water Clusters of Sizes 1, 4, 5, and 6 at the HF/CEP-41G(2d) Level (or HF/aug-cc-PVTZ/6-31G**, Results in Parentheses)[a]

complex	$Zn(H_2O)$	$[Zn(H_2O)_4]^{2+}$	$[Zn(H_2O)_5]^{2+}$	$[Zn(H_2O)_6]^{2+}$
E_{pol} (RVS)	−37.6	−118.7 (−135.3)	−110.8 (−127.5)	−104.3 (−117.5)
E_{CT} (RVS)	−10.9	−28.7 (−9.3)	−24.5 (−6.7)	−21.8 (−4.51)
$(E_{CT}/(E_{pol} + E_{CT})) \times 100$	22.5	19.4 (6.4)	18.1 (5.0)	16.6 (3.7)

[a] Percentage of induction energy due to charge transfer is presented in the last row. All are in units of kcal/mol.

criteria for induced dipole computation is 0.01 D. Molecular dynamics simulations were performed with a 1 fs time step for 500 ps at each perturbation step. Trajectories were saved every 0.1 ps after the first 50 ps equilibration period. The temperature was maintained using the Berendsen weak coupling method at 298 K.[58] The system contained 512 water molecules with one Zn^{2+} ion, and 24.857 Å is the length of each side of the cube.

The absolute free energy was computed from the perturbation steps by using the Bennett acceptance ratio (BAR), a free energy calculation method that utilizes forward and reverse perturbations to minimize variance.[59,60] MD simulations were extended for 2.2 ns (total 2.7 ns) with the final Zn^{2+} parameters, and the resulting trajectory was used in the analysis of the structure and dynamics of water molecules in the first solvation shell. Water molecules separated by a distance less than the first minimum of the Zn^{2+}−O RDF were considered to be in the first solvation shell. The averaged residence time of the first shell water molecules was directly measured by monitoring the entering and exiing events.

IV. Results and Discussion

Contribution of Charge Transfer in Zn^{2+}−Water Complexes. The lack of explicit charge transfer (CT) in AMOEBA presents an interesting challenge. When the CT contribution is significant, despite its limited magnitude in many-body complexes, it may be difficult to capture the overall many-body effect by only considering polarization. Therefore, it is important to investigate the CT contribution to the Zn^{2+}−water interaction energy and its dependence on the system size. To estimate the magnitude of charge transfer, we performed several RVS energy decomposition analyses on complexes up to $[Zn(H_2O)_6]^{2+}$.

We report here complexes that were initially studied by Gresh et al.:[22,61,62] the monoligated $[Zn(H_2O)]^{2+}$ complex and polyligated $[Zn(H_2O)_6]^{2+}$, $[Zn(H_2O)_5(H_2O)]^{2+}$, and $[Zn(H_2O)_4(H_2O)_2]^{2+}$ arrangements (octahedral → pyramidal → tetrahedral first-shell). As we can see in Table 1, the importance of charge transfer relative to polarization varies with the size of the Zn^{2+}−$(H_2O)_n$ complex and depends on the basis set. It makes up a significant portion of induction for a monoligated $[Zn(H_2O)]^{2+}$, and its contribution decreases as the number of ligating water molecules increases to 6. The charge transfer effect appears to be diluted within the entire induction energy (polarization and charge transfer) as the number of water molecules grows in agreement with the previous observation of anticooperative effects.[22,61,62] Note that basis set superposition error (BSSE) is not taken into account. As indicated by Stone,[63] such systematic error can be clearly associated with the charge transfer effect. In contrast to the inverse relationship between CT and water ligation expressed by the zinc cation, the CT contribution associated with anions, such as Cl^-, has been observed to increase as ligation increases.[64] This phenomenon may be due to the asymmetric solvation environment for the anions as well as their modes of water ligation. However, analyses of CT effects are not apparent, as they are found in both induction energy and basis set superposition error.[63] For the largest complex $[Zn(H_2O)_6]^{2+}$, the BSSE amounts to 3.3 kcal/mol. If removed, the relative weight of charge transfer to the total induction reduces from 16.6% (Table 1) to 15.3% at the CEP-31G(2d) level. Using the large aug-cc-PVTZ for water coupled to the 6-31G** basis set for Zn(II), the observed trends are even more pronounced as the relative importance of charge transfer strongly diminishes from 6.4% of the whole induction for $[Zn(H_2O)_4]^{2+}$ to less than 4% for the $[Zn(H_2O)_6]^{2+}$ complex while polarization becomes more dominant. Thus, the magnitude of the CT estimated by *ab initio* methods is greatly dependent on the basis set used. While our results have been obtained at the Hartree−Fock level, recent studies clearly show that correlation acts on induction and leads to greater charge transfer energy.[17,40] For this reason, we computed the induction energies on selected water clusters at both the HF and DFT level using a recently introduced energy decomposition analysis (EDA) technique based on single configuration-interaction (CI) localized fragment orbitals.[65] We indeed find that the CT contribution increases slightly with DFT; however, overall it accounts for less than 20% of the total induction energy for monoligated complexes and presumably would be even less in the bulk water environment.

To gain further insight into the interaction of Zn^{2+} with water, we performed the electron localization function (ELF) analysis. An important asset of the ELF topological analysis is that it provides a clear description of a covalent bond between two atoms as it exhibits a basin between atoms to indicate electron sharing. Here, we have considered several Zn^{2+}−$(water)_n$ complexes, $n = 1-6$. An important discovery from ELF analysis is that a covalent V(Zn,O) is only observed in the monoligated Zn^{2+}−water complex (Figure 1). In that case, we observe a net concentration of electrons between the zinc cation and the water oxygen, a clear sign of covalent bonding (1.9 e^- on the bond). As n increases, the covalent V(Zn,O) feature disappears despite a residual mixing of Zn^{2+} contributions in the oxygen basin. Indeed, as the Zn−O distances increase with n (Figures 2 and 3), the Zn−O bond becomes more ionic as the charge transfer quickly diminishes. Such behavior could be then understood using the subvalence concept.[46] As shown by de Courcy

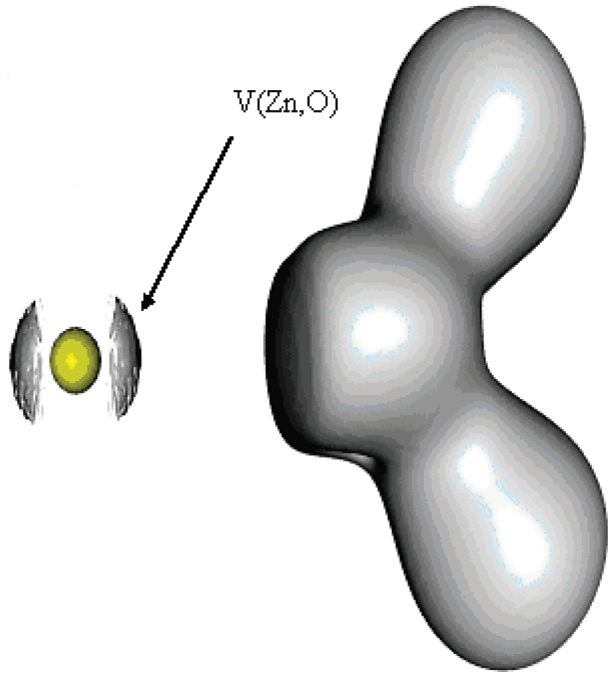

Figure 1. ELF localization domains (basins) for the $Zn^{2+}-H_2O$ complex. A covalent V(Zn,O) basin reflecting electron sharing is observed and reveals the covalent nature of the Zn−O interaction.

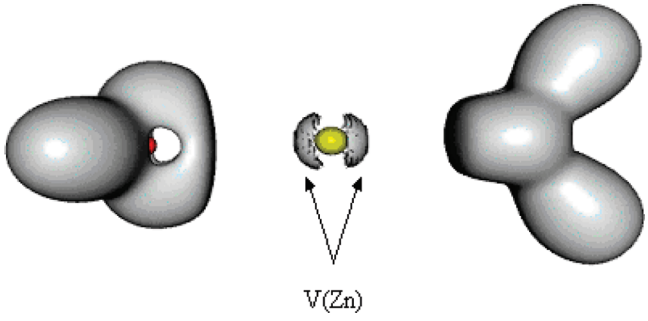

Figure 2. ELF localization domains (basins) for the $Zn^{2+}-(H_2O)_2$ complex. Noncovalent V(Zn) basin are observed describing the deformation of Zn^{2+} outer-shells' density within the fields of the water molecules.

et al.,[4,46] the cation density is split into several "subvalent" domains as its outer shells appear strongly polarized, which explains why covalency is not achieved. If the cation electron density is strongly delocalized toward the oxygen atoms, the center of the basin remains closer to Zn^{2+} (covalent bonding would implicate a polarized bond with a covalent V(Zn,O) basin localized closer to the more electronegative oxygen). ELF results thus suggest that, although the induction in the Zn^{2+}−water monoligated complex is dominated by charge transfer, this is not to the case for n from 2 to 6. In the latter case, the many-body effects are driven by the Zn^{2+} outer shells' plasticity that accommodates the strongly polarized water molecules. The atoms in molecules (AIM) population analysis confirms that such behavior is present in DFT as well as at the MP2 level. As expected (see refs 6 and 40, for example), DFT tends to slightly overbind the complexes as compared to MP2, which clearly gives a better description of the bonding over Hartree−Fock.

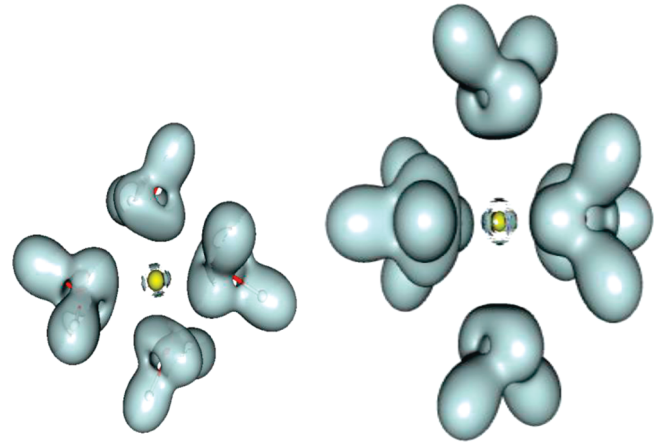

Figure 3. ELF localization domains (basins) for the $Zn^{2+}-(H_2O)_4$ and $Zn^{2+}-(H_2O)_6$ complexes. Again, noncovalent V(Zn) basins are observed.

Table 2. Ion Parameters: Diameter, Well Depth, Polarizability, and Dimensionless Damping Coefficient

ion	R (Å)	ε (kcal/mol)	α (Å^3)	a^a
Zn^{2+}	2.68	0.222	0.260	0.2096
Mg^{2+}	2.94	0.300	0.080	0.0952
Ca^{2+}	3.63	0.350	0.550	0.1585

[a] a is the dimensionless damping coefficient.

To conclude on these various results, we expect that AMOEBA will improve in accuracy with an increase in system size as the charge transfer effect becomes less important and the total induction will be dominated by polarization. In other words, we anticipate the discrepancy between AMOEBA and QM observed in the monoligated water−Zn^{2+} complex to disappear in the condensed phase. This also suggests that an "ad-hoc" inclusion of the charge transfer into the polarization contribution by adjusting the polarization damping scheme (see the Thole model in the Computational Details) is probably not a suitable strategy. Indeed, charge transfer can rapidly vanish, and "polarization only" models overfitted on monoligated complexes to include charge transfer will lead to an overestimated many-body effect in bulk-phase simulation as the polarization would still contain the unphysical charge transfer. Charge transfer should be treated explicitly or included in the van der Waals to a certain extent. In this study, we adopt the latter approach to effectively incorporate the charge transfer in the bulk environment into the vdW interactions.

Accuracy of the AMOEBA Parametrization. The distance-dependent dimer binding energies were used to adjust vdW parameters (R and ε), and the damping factor of polarizability (a) for Zn^{2+} was adjusted to match the CSOV polarization energy. Table 2 lists the final parameters of the Zn^{2+} cation as well as the Mg^{2+} and Ca^{2+} cations parametrized by Jiao et al.[28] that are optimized for the Tinker implementation of AMOEBA. Meanwhile, parameters optimized for a slightly modified implementation of the AMOEBA force field present in Amber which embodies a modified periodic boundary condition treatment of long-range van der Waals are available as well.[29] It should be noted that, although the previously reported parameters for Mg^{2+}

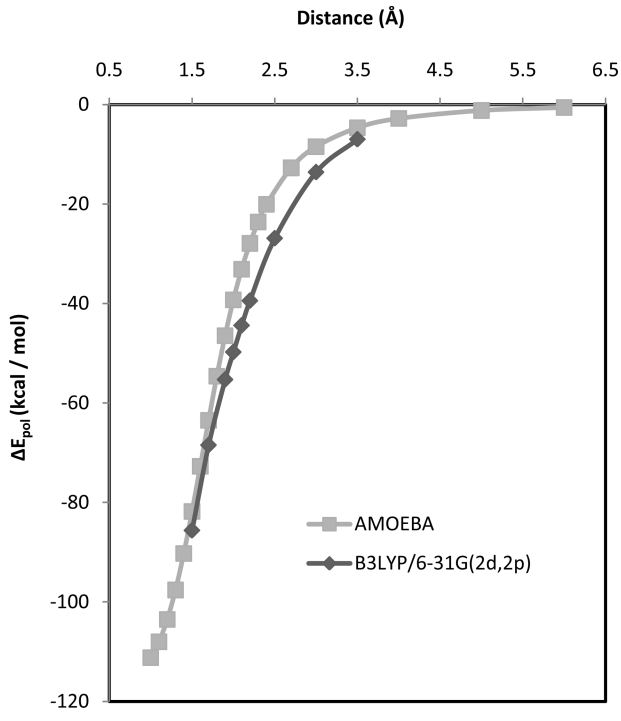

Figure 4. Polarization energy of the zinc and water dimer in the gas phase as a function of separation distance.

and Ca^{2+} contained typographic inconsistencies,[28] results from that work (thermodynamic energy, structural analysis, etc.) are obtained from parameters consistent with Table 2. Figure 4 compares CSOV polarization energy calculations with the AMOEBA polarizable force field as a function of distance between the cation and water. The difference between the two methods is mainly found at distances between 2 and 3 Å, where the charge transfer effect in the two-body system is strong. However, such discrepancy is expected to diminish in bulk water as the charge transfer effect is expected to be less important, as explained above. Comparisons between total binding energies of the AMOEBA polarizable model and *ab initio* calculations are shown in Figure 5. As expected, the interaction energy between 2 and 3.5 Å appears to be underestimated (less negative) compared to the *ab initio* result. The strategy here is, however, not to overfit the AMOEBA model to the monoligated Zn^{2+} complex, as the polarization energy and total interaction energy are already very reasonable considering the relatively simple force field functional form. The AMOEBA association energies for $[Zn(H_2O)_6]^{2+}$, $[Zn(H_2O)_5(H_2O)]^{2+}$, and $[Zn(H_2O)_4(H_2O)_2]_2$ complexes are −334.4, −333.4, and −331.9/−333.7 kcal/mol, respectively. Given that AMOEBA is mainly targeting the condensed phase, the trend observed here is in reasonable agreement with the previous *ab initio* results (−345.3, −341.3, −337.4/−337.8 kcal/mol using CEP 4−31G (2d) basis set; −365.9, −363.3, −360.0/−362.4 kcal/mol using 6-311G** basis set).[62] Our approach is further validated in the condensed-phase hydration properties calculation next.

Evaluation of Zn^{2+} Solvation in Water Using AMOEBA. The hydration free energy is the key quantity describing the thermodynamic stability of an ion in solution. The solvation free energy of zinc in water has been computed from molecular dynamics simulations using free energy perturbation (FEP). Table 3 lists the free energy of hydration for Zn^{2+}, Mg^{2+}, and Ca^{2+} compared with experiment-derived values[66,67] and the results from the quasi-chemical approximation method.[14] The free energy values computed from AMOEBA are closer to those from quasi-chemical approximation (QCA) than to the data interpreted from experimental measurement. In the QCA method, the region around the solute of interest is partitioned into inner and outer shell domains. The inner shell was treated quantum mechanically, while the outer shell was evaluated using a dielectric continuum model. Note that, to decompose the hydration free energy of a neutral ion pair, tetraphenylarsonium tetraphenylborate (TATB) has been most widely chosen as a reference salt, on the basis of the extra thermodynamic assumption that the large and hydrophobic ions do not produce charge-specific solvent ordering effects.[55,66] Our results show better agreement with "experimental values" for Ca^{2+} and Mg^{2+} ions by Schmid et al., who derived the single ion hydration free energy by using the theoretically determined proton hydration free energy as a reference.[67] The hydration free energy for the Zn^{2+} ion computed using AMOEBA is in good agreement with values given by Marcus[66] and Asthagiri et al.,[14] with deviations less than 1.9% and 0.2%, respectively.

Solvent Structure and Dynamics. To characterize the structure of water molecules around the ion, the radial distribution function (RDF) between the Zn^{2+} and oxygen atom of the water molecule has been obtained from the 2.7 ns molecular dynamics simulation (Figure 6). The running integration of Zn−O, which imparts water−ion coordination information, is also plotted. The first minimum in the ion−O RDF is at a distance of 2.85 Å, which can be interpreted as the effective "size" of the complex composed of the ion and first water solvent shell. The running integration indicates a water-coordination number of 6 in the first solvation shell, which is consistent with experimental observations.[68−73] As expected, the zinc cation binds to the first water shell more tightly than other ions, as evident in the more pronounced and narrow first peak as well as the shortest separation, as shown in the ion−O RDFs in Figure 7. Overall, the zinc solvation structure show greater similarity to Mg^{2+} than Ca^{2+}.

The Born theory of ion solvation[74] states that there exists an effective solvation radius, R_B, for each ion such that the solvation free energy of the ion in a dielectric medium is given by

$$\Delta A = -\frac{q^2}{2R_B}\left(1 - \frac{1}{\varepsilon_d}\right)$$

where q is the charge of the ion and ε_d is the dielectric constant of the medium (80 for water). We have calculated the effective radius of zinc on the basis of the Born equation from the solvation free energy obtained from our simulations. Table 4 gives a detailed comparison among Zn^{2+}, Mg^{2+}, and Ca^{2+}. It should be noted, however, that previous studies have shown that ion hydration energy is not symmetric with respect to electronegativity,[27,75,76] as is implied by the Born theory. The first peak of the Zn^{2+}−O RDF is at 1.98 Å, and

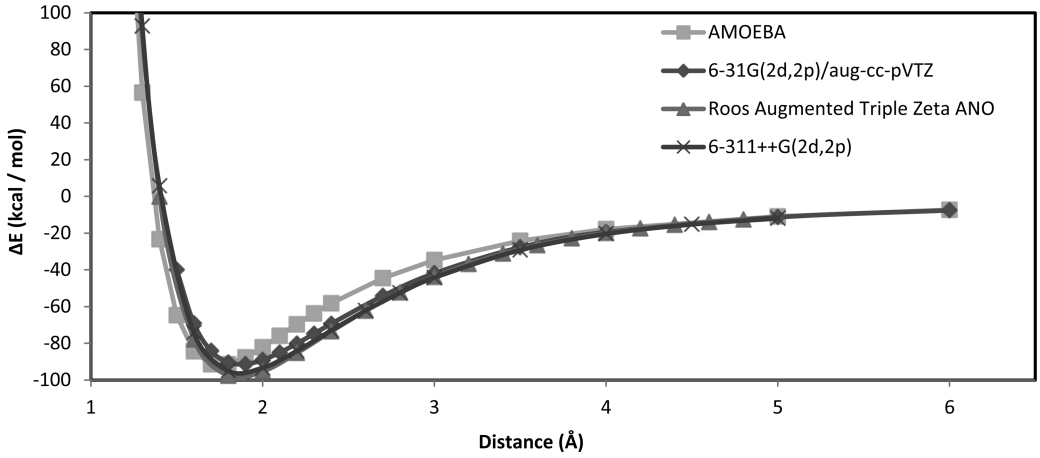

Figure 5. Binding energy of the zinc and water dimer in the gas phase as a function of separation distance. The 6-31G(2d,2p)/aug-cc-pVTZ indicates that 6-31G(2d,2p) was used to represent the Zn^{2+} cation and aug-cc-pVTZ was used to represent the water molecule. Binding energy obtained from the last two basis sets used the same basis sets for both the ion and water.

Table 3. Solvation Free Energy of Zinc in Water[a]

ion	ΔG (kcal/mol)	experimental	quasi-chemical[b]
Zn^{2+}	−458.9(4.4)	−467.7[c]	−460.0
Mg^{2+}	−431.1(2.9)	−435.4[d]	−435.2
Ca^{2+}	−354.9(1.7)	−357.2[d]	−356.6

[a] A 1 mol L^{-1} solution is chosen as the standard state. [b] Ref 14. [c] Ref 66. [d] Ref 67.

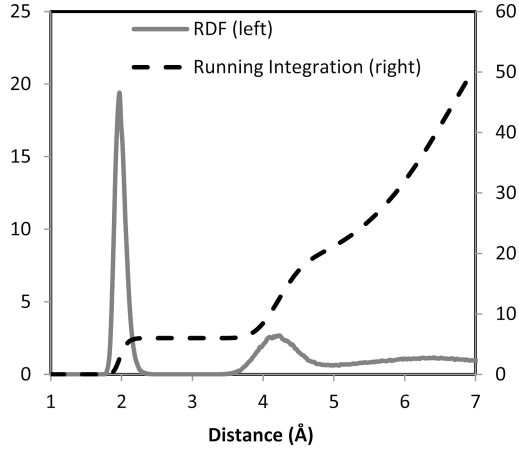

Figure 6. Radial distribution function of Zn^{2+}−O (left axis) and water coordination number (right axis).

the effective Born radius of the cation is calculated to be 1.47 Å. A difference of ∼0.5 Å between the two quantities is consistent with the results of other mono- and divalent metal ions.[27,28,77−79] The difference between the first minimum in the Zn^{2+}−O RDF and the Born radius is 1.38 Å and is consistent with studies of other ions as well.[27,28]

In addition to the RDF, the solvation structure has been analyzed from the distribution of the angles formed by O−ion−O in the first water shell. Figure 8 compares the distribution of angles for Zn^{2+}, Mg^{2+}, and Ca^{2+} cations. With sharp peaks located near 90° and 180°, the distribution of the O−Zn^{2+}−O angle suggests a rigid octahedron geometry with the Zn^{2+} surrounded by six water molecules. Mg^{2+} shares a similar but slightly more flexible geometry, while results for Ca^{2+} suggest a more amorphous structure. Figure 9 shows the dipole moment at each distance (Å)

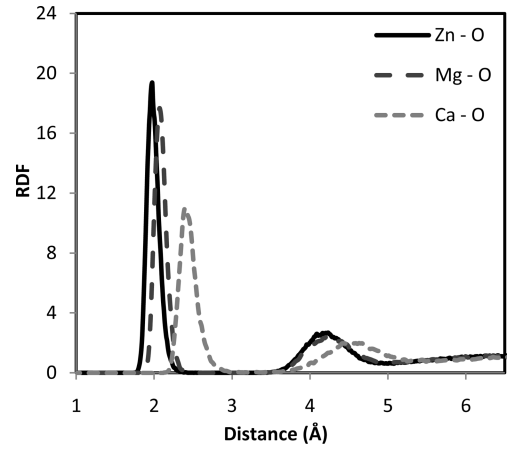

Figure 7. Radial distribution function of divalent cations (Zn^{2+}, Mg^{2+}, and Ca^{2+}) and the oxygen atom in water.

around the ion. Figure 10 is a sample frame from the molecular dynamics simulation to illustrate the octahedron arrangement between the zinc and the first shell water molecules.

Dipole Moment. The average dipole moment of water as a function of distance away from the zinc cation is computed. At the closest distance of 1.9−2.5 Å, water experiences a dipole moment from 3.0 to 3.9 D. Due to the highly organized structure of the first water shell, a "vacuum" space free of water molecules is observed between 2.6 and 3.2 Å away from the cation, also evident in the Zn^{2+}−O RDF. The higher dipole moment of Zn^{2+} relative to bulk water (2.77 D[36]) within the first water shell is consistent with a previous observation of other divalent cations.[28] The dipole moment of water in the first solvation shell of monovalent cations such as K^+ and Na^+, however, is lower than that of bulk water.[55]

Residence Time. We have investigated the lifetime of ion−water coordination by directly examining the average amount of time that a water molecule resides within the first solvation shell. The first solvation shell is determined by the position of the first minimum of the Zn−O RDF. If an oxygen atom is less than 2.85 Å away from the Zn^{2+}, the water is considered to be in the first solvation shell. Cutoff

Table 4. Radii Results for Zn^{2+}, Mg^{2+}, and Ca^{2+} Cations[a]

ion	Born radius (Å)	first peak in ion-O RDF	experimental first peak in ion-O RDF	QM/MM first peak	first minimum in ion-O RDF
Zn^{2+}	1.47	1.98	2.07[b]	2.11−2.18[b]	2.85
Mg^{2+}	1.56[c]	2.07	2.09[d]	2.13[e]	2.95
Ca^{2+}	1.89[c]	2.41	2.41−2.44;2.437;2.46[d]	2.43−2.44[e]	3.23

[a] Born radii, first peak in ion-O RDF with AMOEBA polarizable force field, experimental first peak in ion-O RDF, and first minimum in ion-O RDF are all indicated in Å. [b] Ref 69. [c] Ref 28 [d] Refs 77, 78, and 79. [e] Refs 77, 78.

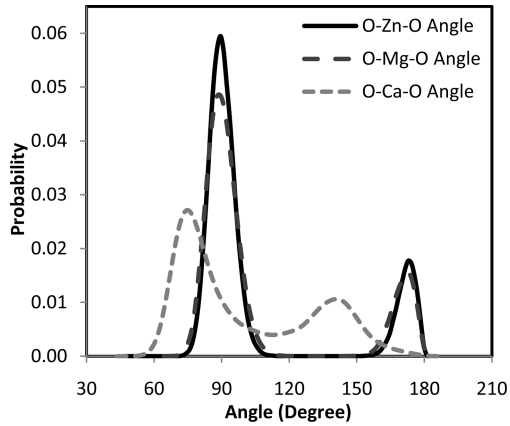

Figure 8. Water−ion−water angle distribution of divalent cations (Zn^{2+}, Mg^{2+}, and Ca^{2+}) and the oxygen atom in water.

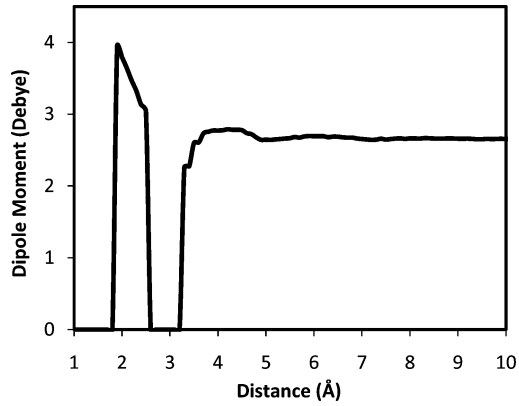

Figure 9. Dipole moment at each distance (Å) around the ion.

distances used for the first solvation shells of Mg^{2+} and Ca^{2+} are 2.95 and 3.23 Å, respectively. In Table 5, coordination numbers and residence times from AMOEBA simulations are compared with experimental values for Zn^{2+}, Mg^{2+}, and Ca^{2+}.[20,80−86] The Zn^{2+} to water-proton dynamics are studied with quasi-elastic neutron scattering methods (QENS) as described by Salmon et al.[80] The water residence times directly sampled from the MD simulations are in better agreement with experimental results than those previously inferred from the time correlation function of the instantaneous first shell coordination number.[28] According to AMOEBA simulations, the residence time in the first solvation shell around Zn^{2+} is at least 2 ns, and the water molecules around Ca^{2+} have a lifetime on the order of several picoseconds, both of which are within the experimental ranges. For Mg^{2+}, experimental results suggest that water molecules could live up to a few microseconds, while the simulations using AMOEBA indicate a residence time similar

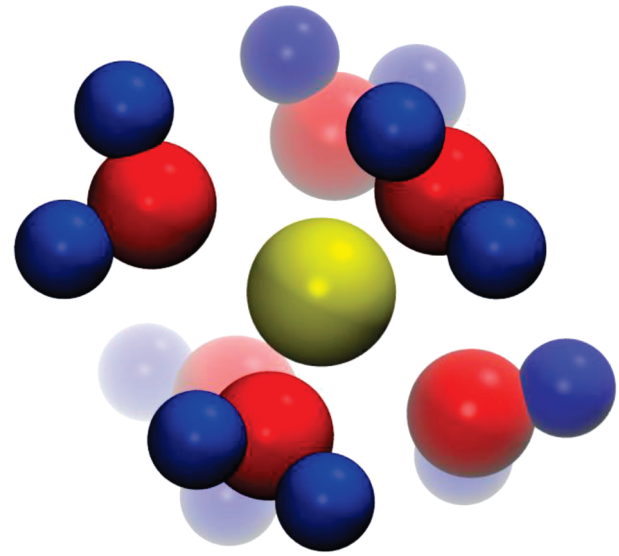

Figure 10. First solvation shell around the Zn^{2+} ion.

Table 5. Coordination Number, Experimental Coordination Number, Residence Time, Experimental Residence Time, and QM/MM Residence Times for Each Type of Divalent Cations.

ion	coordination number	exp. coordination number	residence time (s)	exp residence time (s)
Zn^{2+}	6	6[a]	2.2×10^{-9}	10^{-10} to 10^{-9}[b]
Mg^{2+}	6	6[c]	1.9×10^{-9}	2×10^{-6} to 10^{-5}[d,e]
Ca^{2+}	7.3	7.2 ± 1.2[f]	1.33×10^{-10}	$<10^{-10}$ to 10^{-7}[e]

[a] Refs 68−73. [b] Refs 80 and 20. [c] Ref 85. [d] Refs 81. [e] Refs 84, 82 and references within, and 83. [f] Ref 86.

to that of Zn^{2+}. Classical fixed-charge molecular mechanic methods suggest a residence time of 146 ps[87] for water around Zn^{2+}, while quantum mechanical methods have not attained simulation times long enough to observe the exchange of water molecules in the first shell.[68,88] The calculated water residence times are consistent with the analyses of the radial distribution function and water angle distribution. A longer residence time is accompanied by a more ordered and closely packed water structure near the cation.

Conclusions

We showed in this contribution that AMOEBA was able to provide a reasonably accurate description of Zn^{2+} interaction with water, especially in the bulk water environment. We explained in detail one of the reasons for such good performance—the *ab initio* calculations demonstrated that the relative importance of charge transfer diminishes as the number of water molecule increases, a sign of anticooperativity. We have established a fitting strategy for induction:

charge transfer can be included in the pairwise dispersion in the van der Waals contribution; incorporation of charge transfer into polarization would lead to an overestimation of the many-body effects. Despite the difficulty involved with the AMOEBA model reproducing the binding energy of the monoligated Zn^{2+}−water complex, which exhibits nonclassical covalent bonding as shown by ELF topological analysis, AMOEBA is able to afford robust estimation of the hydration free energy along with reasonable solvation structure and dynamics. The current and previous studies suggest that the classical polarizable multipole-based AMOEBA is an effective tool for modeling ions in bulk solution, as good relative solvation free energies, structures, and dynamic properties have been obtained for a range of mono- and divalent cations. The work clearly demonstrates the need for "interpretative" *ab initio* techniques (ELF, EDA methods) in order to follow a bottom-up approach going from the gas-phase *ab initio* calculations to condensed-phase MD simulations. In addition, the zinc model developed in this work opens the door for future study of zinc-containing metalloproteins. Further investigation is necessary to determine whether the presence of negatively charged species interacting with Zn^{2+} would require an explicit consideration of charge transfer contribution in the classical energy function.

Acknowledgment. This research was supported by grants from the National Institute of General Medical Sciences (R01GM079686) and the Robert A. Welch Foundation (F-1691) to P.R. This work was also supported by the French National Research Agency (ANR) on project LASIHMODo (ANR-08-BLAN-0158-01) (J.-P.P.). Some computations have been carried out at GENCI IDRIS (F. 91403 Orsay, France) and CRIHAN (F. 76800 Saint-Etienne-de-Rouvray, France) supercomputer centers.

Supporting Information Available: Symmetry adapted perturbation theory (SAPT) results for the water−Zn(II) complex. This information is available free of charge via the Internet at http://pubs.acs.org/.

References

(1) Keilin, D.; Mann, T. Carbonic anhydrase. Purification and nature of the enzyme. *Biochem. J.* **1940**, *34*, 1163–1176.

(2) Maynard, A. T.; Covell, D. G. Reactivity of zinc finger cores: Analysis of protein packing and electrostatic screening. *J. Am. Chem. Soc.* **2001**, *123*, 1047–1058.

(3) Lipscomb, W. N.; Strater, N. Recent advances in zinc enzymology. *Chem. Rev. (Washington, DC, U. S.)* **1996**, *96*, 2375–2433.

(4) De Courcy, B.; Gresh, N.; Piquemal, J. P. Importance of lone pair interactions/redistribution in hard and soft ligands within the active site of alcohol dehydrogenase Zn-metalloenzyme: Insights from electron localization function. *Interdisc. Sci.: Comput. Life Sci.* **2009**, *1*, 55–60.

(5) Gresh, N.; Garmer, D. R. Comparative binding energetics of Mg2+, Ca2+, Zn2+, and Cd2+ to biologically relevant ligands: Combined ab initio SCF supermolecule and molecular mechanics investigation. *J. Comput. Chem.* **1996**, *17*, 1481–1495.

(6) Rayon, V. M.; Valdes, H.; Diaz, N.; Suarez, D. Monoligand Zn(II) complexes: Ab initio benchmark calculations and comparison with density functional theory methodologies. *J. Chem. Theory Comput.* **2008**, *4*, 243–256.

(7) Amin, E. A.; Truhlar, D. G. Zn coordination chemistry: Development of benchmark suites for geometries, dipole moments, and bond dissociation energies and their use to test and validate density functionals and molecular orbital theory. *J. Chem. Theory Comput.* **2008**, *4*, 75–85.

(8) Warshel, A.; Levitt, M. Theoretical studies of enzymic reactions - dielectric, electrostatic and steric stabilization of carbonium-ion in reaction of lysozyme. *J. Mol. Biol.* **1976**, *103*, 227–249.

(9) Estiu, G.; Suarez, D.; Merz, K. M. Quantum mechanical and molecular dynamics simulations of ureases and Zn beta-lactamases. *J. Comput. Chem.* **2006**, *27*, 1240–1262.

(10) Friesner, R. A.; Guallar, V. Ab initio quantum chemical and mixed quantum mechanics/molecular mechanics (QM/MM) methods for studying enzymatic catalysis. *Annu. Rev. Phys. Chem.* **2005**, *56*, 389–427.

(11) Ryde, U. Combined quantum and molecular mechanics calculations on metalloproteins. *Curr. Opin. Chem. Biol.* **2003**, *7*, 136–142.

(12) Tuccinardi, T.; Martinelli, A.; Nuti, E.; Carelli, P.; Balzano, F.; Uccello-Barretta, G.; Murphy, G.; Rossello, A. Amber force field implementation, molecular modelling study, synthesis and MMP-1/MMP-2 inhibition profile of (R)and (S)-N-hydroxy-2-(N-isopropoxybiphenyl-4-ylsulfonamido)-3-methylbutanamides. *Bioorg. Med. Chem.* **2006**, *14*, 4260–4276.

(13) Yuan-Ping, P. Successful molecular dynamics simulation of two zinc complexes bridged by a hydroxide in phosphotriesterase using the cationic dummy atom method. *Proteins: Struct., Funct., Genet.* **2001**, *45*, 183–189.

(14) Asthagiri, D.; Pratt, L. R.; Paulaitis, M. E.; Rempe, S. B. Hydration structure and free energy of biomolecularly specific aqueous dications, including Zn2+ and first transition row metals. *J. Am. Chem. Soc.* **2004**, *126*, 1285–1289.

(15) Rogers, D. M.; Beck, T. L. Quasichemical and structural analysis of polarizable anion hydration. *J. Chem. Phys.* **2010**, *132*, 014505.

(16) Gresh, N.; Cisneros, G. A.; Darden, T. A.; Piquemal, J. P. Anisotropic, polarizable molecular mechanics studies of inter- and intramoecular interactions and ligand-macromolecule complexes. A bottom-up strategy. *J. Chem. Theory Comput.* **2007**, *3*, 1960–1986.

(17) Cisneros, G. A.; Darden, T. A.; Gresh, N.; Pilmé, J.; Reinhardt, P.; Parisel, O.; Piquemal, J. P. Design Of Next Generation Force Fields From AB Initio Computations: Beyond Point Charges Electrostatics. In *Multi-scale Quantum Models for Biocatalysis* Springer: Netherlands, 2009; Vol. 7, pp 137−172.

(18) Ren, P. Y.; Ponder, J. W. Consistent treatment of inter- and intramolecular polarization in molecular mechanics calculations. *J. Comput. Chem.* **2002**, *23*, 1497–1506.

(19) de Courcy, B.; Piquemal, J. P.; Gresh, N. Energy Analysis of Zn Polycoordination in a Metalloprotein Environment and of the Role of a Neighboring Aromatic Residue. What Is the Impact of Polarization. *J. Chem. Theory Comput.* **2008**, *4*, 1659–1668.

(20) Roux, C.; Gresh, N.; Perera, L.; Piquemal, J.; Salmon, L. Binding of 5-phospho-D-arabinonohydroxamate and 5-phos-

pho-D-arabinonate inhibitors to zinc phosphomannose isomerase from Candida albicans studied by polarizable molecular mechanics and quantum mechanics. *J. Comput. Chem.* **2007**, *28*, 938–957.

(21) Jenkins, L. M. M.; Hara, T.; Durell, S.; Hayashi, R.; Inman, J.; Piquemal, J.; Gresh, N.; Appella, E. Specificity of acyl transfer from 2-mercaptobenzamide thioesters to the HIV-1 nucleocapsid protein. *J. Am. Chem. Soc.* **2007**, *129*, 11067–11078.

(22) Gresh, N.; Piquemal, J.; Krauss, M. Representation of Zn(II) complexes in polarizable molecular mechanics. Further refinements of the electrostatic and short-range contributions. Comparisons with parallel ab initio computations. *J. Comput. Chem.* **2005**, *26*, 1113–1130.

(23) Antony, J.; Piquemal, J. P.; Gresh, N. Complexes of thiomandelate and captopril mercaptocarboxylate inhibitors to metallo-beta-lactamase by polarizable molecular mechanics. Validation on model binding sites by quantum chemistry. *J. Comput. Chem.* **2005**, *26*, 1131–1147.

(24) Jiao, D.; Golubkov, P. A.; Darden, T. A.; Ren, P. Calculation of protein-ligand binding free energy by using a polarizable potential. *Proc. Natl. Acad. Sci. U. S. A.* **2008**, *105*, 6290–6295.

(25) Jiao, D.; Zhang, J. J.; Duke, R. E.; Li, G. H.; Schnieders, M. J.; Ren, P. Y. Trypsin-Ligand Binding Free Energies from Explicit and Implicit Solvent Simulations with Polarizable Potential. *J. Comput. Chem.* **2009**, *30*, 1701–1711.

(26) Ponder, J. W.; Wu, C. J.; Ren, P. Y.; Pande, V. S.; Chodera, J. D.; Schnieders, M. J.; Haque, I.; Mobley, D. L.; Lambrecht, D. S.; DiStasio, R. A.; Head-Gordon, M.; Clark, G. N. I.; Johnson, M. E.; Head-Gordon, T. Current Status of the AMOEBA Polarizable Force Field. *J. Phys. Chem. B* **2010**, *114*, 2549–2564.

(27) Grossfield, A. Dependence of ion hydration on the sign of the ion's charge. *J. Chem. Phys.* **2005**, *122*, 024506.

(28) Jiao, D.; King, C.; Grossfield, A.; Darden, T. A.; Ren, P. Y. Simulation of Ca2+ and Mg2+ solvation using polarizable atomic multipole potential. *J. Phys. Chem. B* **2006**, *110*, 18553–18559.

(29) Piquemal, J. P.; Perera, L.; Cisneros, G. A.; Ren, P. Y.; Pedersen, L. G.; Darden, T. A. Towards accurate solvation dynamics of divalent cations in water using the polarizable amoeba force field: From energetics to structure. *J. Chem. Phys.* **2006**, *125*, 054511.

(30) Bagus, P. S.; Illas, F. Decomposition of the chemisorption bond by constrained variations - Order of the variations and construction of the variational spaces. *J. Chem. Phys.* **1992**, *96*, 8962–8970.

(31) Stevens, W. J.; Fink, W. H. Frozen fragment reduced variational space analysis of hydrogen-bonding interactions - Application to the water dimer. *Chem. Phys. Lett.* **1987**, *139*, 15–22.

(32) Jeziorski, B.; Moszynski, R.; Szalewicz, K. Perturbation-theory approach to intermolecular potential-energy surfaces of van-der-Waals complexes. *Chem. Rev. (Washington, DC, U. S.)* **1994**, *94*, 1887–1930.

(33) Becke, A. D.; Edgecombe, K. E. A simple measure of electron localization in atomic and molecular-systems. *J. Chem. Phys.* **1990**, *92*, 5397–5403.

(34) Silvi, B.; Savin, A. Classification of chemical-bonds based on topological analysis of electron localization functions. *Nature* **1994**, *371*, 683–686.

(35) Frisch, M. J.; Trucks, G. W.; Schlegel, H. B.; Scuseria, G. E.; Robb, M. A.; Cheeseman, J. R.; Montgomery, J. A., Jr.; Vreven, T.; Kudin, K. N.; Burant, J. C.; Millam, J. M.; Iyengar, S. S.; Tomasi, J.; Barone, V.; Mennucci, B.; Cossi, M.; Scalmani, G.; Rega, N.; Petersson, G. A.; Nakatsuji, H.; Hada, M.; Ehara, M.; Toyota, K.; Fukuda, R.; Hasegawa, J.; Ishida, M.; Nakajima, T.; Honda, Y.; Kitao, O.; Nakai, H.; Klene, M.; Li, X.; Knox, J. E.; Hratchian, H. P.; Cross, J. B.; Bakken, V.; Adamo, C.; Jaramillo, J.; Gomperts, R.; Stratmann, R. E.; Yazyev, O.; Austin, A. J.; Cammi, R.; Pomelli, C.; Ochterski, J. W.; Ayala, P. Y.; Morokuma, K.; Voth, G. A.; Salvador, P.; Dannenberg, J. J.; Zakrzewski, V. G.; Dapprich, S.; Daniels, A. D.; Strain, M. C.; Farkas, O.; Malick, D. K.; Rabuck, A. D.; Raghavachari, K.; Foresman, J. B.; Ortiz, J. V.; Cui, Q.; Baboul, A. G.; Clifford, S.; Cioslowski, J.; Stefanov, B. B.; Liu, G.; Liashenko, A.; Piskorz, P.; Komaromi, I.; Martin, R. L.; Fox, D. J.; Keith, T.; Al-Laham, M. A.; Peng, C. Y.; Nanayakkara, A.; Challacombe, M.; Gill, P. M. W.; Johnson, B.; Chen, W.; Wong, M. W.; Gonzalez, C.; Pople, J. A. *Gaussian 03*, Revision D.01; Gaussian, Inc.: Wallingford, CT, 2004.

(36) Ren, P. Y.; Ponder, J. W. Polarizable atomic multipole water model for molecular mechanics simulation. *J. Phys. Chem. B* **2003**, *107*, 5933–5947.

(37) Ren, P. Y.; Ponder, J. W. Temperature and pressure dependence of the AMOEBA water model. *J. Phys. Chem. B* **2004**, *108*, 13427–13437.

(38) Dunning, T. H. Gaussian-Basis Sets for Use in Correlated Molecular Calculations. 1. The Atoms Boron through Neon and Hydrogen. *J. Chem. Phys.* **1989**, *90*, 1007–1023.

(39) Helgaker, T.; Jørgensen, P.; Olsen, J.; Ruud, K.; Andersen, T.; Bak, K. L.; Bakken, V.; Christiansen, O.; Dahle, P.; Dalskov, E. K.; Enevoldsen, T.; Heiberg, H.; Hettema, H.; Jonsson, D.; Kirpekar, S.; Kobayashi, R.; Koch, H.; Mikkelsen, K. V.; Norman, P.; Packer, M. J.; Saue, T.; Taylor, P. R.; Vahtras, O.; Jensen, H. J. A.; Ågren, H. *Dalton, an Ab Initio Electronic Structure Program*, release 1.0, 1997.

(40) Piquemal, J.; Marquez, A.; Parisel, O.; Giessner-Prettre, C. A CSOV study of the difference between HF and DFT intermolecular interaction energy values: The importance of the charge transfer contribution. *J. Comput. Chem.* **2005**, *26*, 1052–1062.

(41) Becke, A. D. Density-Functional Exchange-Energy Approximation with Correct Asymptotic-Behavior. *Phys. Rev. A* **1988**, *38*, 3098–3100.

(42) Lee, C. T.; Yang, W. T.; Parr, R. G. Development of the Colle-Salvetti Correlation-Energy Formula into a Functional of the Electron-Density. *Phys. Rev. B* **1988**, *37*, 785–789.

(43) Gordon, M. S.; Schmidt, M. W., Advances in electronic structure theory: GAMESS a decade later. In *Theory and Applications of Computational Chemistry, the first forty years*, Dykstra, C. E., Frenking, G., Kim, K. S., Scuseria, G. E., Ed.; Elsevier: Amsterdam, 2005.

(44) Stevens, W. J.; Basch, H.; Krauss, M. Compact Effective Potentials and Efficient Shared-Exponent Basis-Sets for the 1st-Row and 2nd-Row Atoms. *J. Chem. Phys.* **1984**, *81*, 6026–6033.

(45) Savin, A.; Nesper, R.; Wengert, S.; Fassler, T. F. ELF: The electron localization function. *Angew. Chem., Int. Ed. Engl.* **1997**, *36*, 1809–1832.

(46) de Courcy, B.; Pedersen, L. G.; Parisel, O.; Gresh, N.; Silvi, B.; Pilme, J.; Piquemal, J. P. Understanding Selectivity of Hard and Soft Metal Cations within Biological Systems Using

the Subvalence Concept. 1. Application to Blood Coagulation: Direct Cation-Protein Electronic Effects versus Indirect Interactions through Water Networks. *J. Chem. Theory Comput.* **2010**, *6*, 1048–1063.

(47) Piquemal, J. P.; Pilme, J.; Parisel, O.; Gerard, H.; Fourre, I.; Berges, J.; Gourlaouen, C.; De La Lande, A.; Van Severen, M. C.; Silvi, B. What can be learnt on biologically relevant systems from the topological analysis of the electron localization function. *Int. J. Quantum Chem.* **2008**, *108*, 1951–1969.

(48) Pilme, J.; Piquemal, J. P. Advancing beyond charge analysis using the electronic localization function: Chemically intuitive distribution of electrostatic moments. *J. Comput. Chem.* **2008**, *29*, 1440–1449.

(49) Noury, S.; Krokidis, X.; Fuster, F.; Silvi, B. Computational tools for the electron localization function topological analysis. *Comput. Chem.* **1999**, *23*, 597–604.

(50) Claverie, P. *Intermolecular Interactions: From Diatomics to Biopolymers*; Wiley: New York, 1978; Vol. 1.

(51) Kutzelnigg, W. The primitive wavefunction in the theory of intermolecular interactions. *J. Chem. Phys.* **1980**, *73*, 343–359.

(52) Reinhardt, P.; Piquemal, J.-P. *Int. J. Quant. Chem.* **2009**, *109*, 3259–3267.

(53) Halgren, T. A. Representation of van der Waals (vdW) interactions in molecular mechanics force-fields - potential form, combination rules, and vdW parameters. *J. Am. Chem. Soc.* **1992**, *114*, 7827–7843.

(54) Masia, M.; Probst, M.; Rey, R. On the performance of molecular polarization methods. II. Water and carbon tetrachloride close to a cation. *J. Chem. Phys.* **2005**, *123*, 164505.

(55) Grossfield, A.; Ren, P. Y.; Ponder, J. W. Ion solvation thermodynamics from simulation with a polarizable force field. *J. Am. Chem. Soc.* **2003**, *125*, 15671–15682.

(56) Ponder, J. *TINKER: Software Tools for Molecular Design*, version 5.0; Washington University School of Medicine: Saint Louis, MO, 2009.

(57) Sagui, C.; Pedersen, L. G.; Darden, T. A. Towards an accurate representation of electrostatics in classical force fields: Efficient implementation of multipolar interactions in biomolecular simulations. *J. Chem. Phys.* **2004**, *120*, 73–87.

(58) Berendsen, H. J. C.; Postma, J. P. M.; van Gunsteren, W. F.; DiNola, A.; Haak, J. R. Molecular Dynamics with Coupling to an External Bath. *J. Chem. Phys.* **1984**, *81*, 3684–3690.

(59) Bennett, C. H. Efficient Estimation of Free-Energy Differences from Monte-Carlo Data. *J. Comput. Phys.* **1976**, *22*, 245–268.

(60) Shirts, M. R.; Bair, E.; Hooker, G.; Pande, V. S. Equilibrium free energies from nonequilibrium measurements using maximum-likelihood methods. *Phys. Rev. Lett.* **2003**, *91*, 140601−1–4.

(61) Gresh, N. Energetics of Zn2+ Binding to a Series of Biologically Relevant Ligands - a Molecular Mechanics Investigation Grounded on Ab-Initio Self-Consistent-Field Supermolecular Computations. *J. Comput. Chem.* **1995**, *16*, 856–882.

(62) Tiraboschi, G.; Gresh, N.; Giessner-Prettre, C.; Pedersen, L. G.; Deerfield, D. W. Parallel ab initio and molecular mechanics investigation of polycoordinated Zn(II) complexes with model hard and soft ligands: Variations of binding energy and of its components with number and charges of ligands. *J. Comput. Chem.* **2000**, *21*, 1011–1039.

(63) Stone, A. J. *The Theory of Intermolecular Forces*; Oxford University Press: New York, 1997.

(64) Zhao, Z.; Rogers, D. M.; Beck, T. L. Polarization and charge transfer in the hydration of chloride ions. *J. Chem. Phys.* **2010**, *132*, 014502.

(65) Reinhardt, P.; Piquemal, J.; Savin, A. Fragment-Localized Kohn-Sham Orbitals via a Singles Configuration-interaction Procedure and Application to Local Properties and Intermolecular Energy Decomposition Analysis. *J. Chem. Theory Comput.* **2008**, *4*, 2020–2029.

(66) Marcus, Y. A Simple Empirical-Model Describing the Thermodynamics of Hydration of Ions of Widely Varying Charges, Sizes, and Shapes. *Biophys. Chem.* **1994**, *51*, 111–127.

(67) Schmid, R.; Miah, A. M.; Sapunov, V. N. A new table of the thermodynamic quantities of ionic hydration: values and some applications (enthalpy-entropy compensation and Born radii). *Phys. Chem. Chem. Phys.* **2000**, *2*, 97–102.

(68) Mohammed, A. M.; Loeffler, H. H.; Inada, Y.; Tanada, K.-i.; Funahashi, S. Quantum mechanical/molecular mechanical molecular dynamic simulation of zinc(II) ion in water. *J. Mol. Liq.* **2005**, *119*, 55–62.

(69) D'Angelo, P.; Barone, V.; Chillemi, G.; Sanna, N.; Meyer-Klaucke, W.; Pavel, N. V. Hydrogen and Higher Shell Contributions in Zn2+, Ni2+, and Co2+ Aqueous Solutions: An X-ray Absorption Fine Structure and Molecular Dynamics Study. *J. Am. Chem. Soc.* **2002**, *124*, 1958–1967.

(70) Obst, S.; Bradaczek, H. Molecular dynamics simulations of zinc ions in water using CHARMM. *J. Mol. Model.* **1997**, *3*, 224–232.

(71) Kuzmin, A.; Obst, S.; Purans, J. X-ray absorption spectroscopy and molecular dynamics studies of Zn2+ hydration in aqueous solutions. *J. Phys.: Condens. Matter* **1997**, *9*, 10065–10078.

(72) Marini, G. W.; Texler, N. R.; Rode, B. M. Monte Carlo simulations of Zn(II) in water including three-body effects. *J. Phys. Chem.* **1996**, *100*, 6808–6813.

(73) Yongyai, Y. P.; Kokpol, S.; Rode, B. M. Zinc Ion in Water - Intermolecular Potential with Approximate 3-Body Correction and Monte-Carlo Simulation. *Chem. Phys.* **1991**, *156*, 403–412.

(74) Born, M. Volumen und Hydratationswärme der Ionen. *Z. Phys. A Hadrons Nuclei* **1920**, *1*, 45–48.

(75) Garde, S.; Hummer, G.; Paulaitis, M. E. Free energy of hydration of a molecular ionic solute: Tetramethylammonium ion. *J. Chem. Phys.* **1998**, *108*, 1552–1561.

(76) Rajamani, S.; Ghosh, T.; Garde, S. Size dependent ion hydration, its asymmetry, and convergence to macroscopic behavior. *J. Chem. Phys.* **2004**, *120*, 4457–4466.

(77) Naor, M. M.; Van Nostrand, K.; Dellago, C. Car-Parrinello molecular dynamics simulation of the calcium ion in liquid water. *Chem. Phys. Lett.* **2003**, *369*, 159–164.

(78) Badyal, Y. S.; Barnes, A. C.; Cuello, G. J.; Simonson, J. M. Understanding the effects of concentration on the solvation structure of Ca2+ in aqueous solutions. II: Insights into longer range order from neutron diffraction isotope substitution. *J. Phys. Chem. A* **2004**, *108*, 11819–11827.

(79) Jalilehvand, F.; Spangberg, D.; Lindqvist-Reis, P.; Hermansson, K.; Persson, I.; Sandstrom, M. Hydration of the calcium ion. An EXAFS, large-angle X-ray scattering, and molecular dynamics simulation study. *J. Am. Chem. Soc.* **2001**, *123*, 431–441.

(80) Salmon, P. S.; Bellissentfunel, M. C.; Herdman, G. J. The Dynamics of Aqueous Zn-2+ Solutions - a Study Using Incoherent Quasi-Elastic Neutron-Scattering. *J. Phys.: Condens. Matt.* **1990**, *2*, 4297–4309.

(81) Neely, J.; Connick, R. Rate of water exchange from hydrated magnesium ion. *J. Am. Chem. Soc.* **1970**, *92*, 3476–3478.

(82) Friedman, H. Hydration complexes - some firm results and some pressing questions. *Chemica Scripta* **1985**, *25*, 42–48.

(83) Ohtaki, H.; Radnai, T. Structure and dynamics of hydrated ions. *Chem. Rev. (Washington, DC, U. S.)* **1993**, *93*, 1157–1204.

(84) Helm, L.; Merbach, A. E. Water exchange on metal ions: experiments and simulations. *Coord. Chem. Rev.* **1999**, *187*, 151–181.

(85) Caminiti, R.; Licheri, G.; Piccaluga, G.; Pinna, G. X-ray-diffraction study of a 3-ion aqueous-solution. *Chem. Phys. Lett.* **1977**, *47*, 275–278.

(86) Lightstone, F. C.; Schwegler, E.; Allesch, M.; Gygi, F.; Galli, G. A first-principles molecular dynamics study of calcium in water. *ChemPhysChem* **2005**, *6*, 1745–1749.

(87) Fatmi, M. Q.; Hofer, T. S.; Randolf, B. R.; Rode, B. M. An extended ab initio QM/MM MD approach to structure and dynamics of Zn(II) in aqueous solution. *J. Chem. Phys.* **2005**, *123*, 054514−8.

(88) Fatmi, M. Q.; Hofer, T. S.; Randolf, B. R.; Rode, B. M. Temperature Effects on the Structural and Dynamical Properties of the Zn(II)-Water Complex in Aqueous Solution: A QM/MM Molecular Dynamics Study. *J. Phys. Chem. B* **2006**, *110*, 616–621.

CT100091J